IEEE Access
Multidisciplinary | Rapid Review | Open Access Journal

Received June 17, 2020, accepted July 1, 2020, date of publication July 20, 2020, date of current version August 7, 2020.

Digital Object Identifier 10.1109/ACCESS.2020.3010539

A Piezoelectric Bellows Round-Window Driver (PBRD) for Middle-Ear Implants

DONG HO SHIN[1], KI WOONG SEONG[2], HIDEKO HEIDI NAKAJIMA[3], SUNIL PURIA[3], AND JIN-HO CHO[1], (Senior Member, IEEE)

[1]Institute of Biomedical Engineering Research, Kyungpook National University, Daegu 41944, South Korea
[2]Department of Biomedical Engineering, Kyungpook National University Hospital, Daegu 41944, South Korea
[3]Department of Otolaryngology, Harvard Medical School, Massachusetts Eye and Ear, Boston, MA 02114, USA

Corresponding author: Jin-Ho Cho (jhcho@ee.knu.ac.kr)

This work was supported in part by the Korea Health Industry Development Institute (KHIDI) through the Korea Health Technology Research and Development Project, funded by the Ministry of Health and Welfare, South Korea, under Grant HI18C1892; and in part by a National Research Foundation of Korea (NRF) grant funded by the Korean Government (MSIP) under Grant NRF-2019R1C1C1006176.

ABSTRACT We describe a new implantable hearing-aid output device, a piezoelectric bellows round-window driver (PBRD), which is expected to be unaffected by external magnetic fields. The core elements of the PBRD are a piezoelectric element and a gold-coated copper bellows of low stiffness that transmits piezoelectric displacements, without significant attenuation, to the round window (RW). We analyzed structural and mechanical vibrations when confirming bellows transmission efficiency using a finite element model simulation. The PBRD was bench-tested under no-load conditions to determine its frequency response characteristics. We compared the outputs of the PBRD and a commercial floating-mass transducer in situ in human cadaveric temporal bones with responses measured using a laser Doppler vibrometer. PBRD outputs were excellent at both low (0.1–0.7 kHz) and high (2–16 kHz) frequencies; thus, the PBRD has the potential to compensate for conductive and/or sensorineural hearing loss. The frequency-response performance of the PBRD is better than that of conventional RW drivers (actuators or transducers).

INDEX TERMS Piezoelectric bellows round-window driver (PBRD), middle-ear implants, finite element analysis, human temporal bone, conductive or sensorineural hearing loss.

I. INTRODUCTION

Middle-ear implants that transmit vibrations using small transducers have been widely employed to compensate for conductive and/or sensorineural hearing loss [1]–[9]. Middle-ear implants allow high-quality speech discrimination, and many reports have indicated that patients favor implants over conventional hearing aids [10]–[13]. The floating-mass transducer (FMT) of Vibrant Soundbridge (VSB, MED-El Inc.) is a middle-ear implant clinically used and studied [14]–[16]. Usually, the FMT is installed onto the short or long process of the incus, and stimulates the cochlea through the oval window [17]. However, this is not possible if the ossicular chain is lost to disease or deformity. Thus, FMTs have been placed in the round window (RW) niche [18]–[20]. However, the low-frequency (below 1 kHz) output to the RW is poor [21], [22]. Also, as the FMT contains a magnet and a coil, it may be affected by environmental magnetic fields.

The implantable RW-driving tri-coil bellows transducer (TCBT) of Shin *et al*. features three coils, a three-pole magnet, and a miniaturized bellows [23]. With the TCBT, the poor low-frequency output characteristics of the FMT can be avoided. This is due to the TCBT housing being fixed, not floating, which is associated with excellent output characteristics from 0.1 to 10 kHz. The TCBT is small (diameter 1.75 mm and length 2.3 mm) and thus easy to implant. The three-pole magnet minimizes (but does not eliminate) the effects of environmental magnetic fields; both the FMT and TCBT are likely to be affected by strong fields such as from magnetic resonance imaging (MRI) [24], [25]. Indeed, the MRI safety of middle-ear output devices is one of the most important issues to resolve to significantly improve the practicality of middle-ear implants. Therefore,

The associate editor coordinating the review of this manuscript and approving it for publication was Yizhang Jiang.

a transducer exhibiting good frequency characteristics and immunity to environmental magnetic fields is required.

Here, we present a novel RW-drive transducer, the piezoelectric bellows RW driver (PBRD), which has a vibrating bellows similar in exterior design to our earlier TCBT [23], but incorporates a piezoelectric element that is unaffected by external magnetic fields. Finite-element analysis (FEA) showed that our device using a bellows has superior vibration-transmission efficiency as compared to a version with a flat circular membrane. We built and bench-tested our PBRD, in terms of output characteristics, under no-load conditions. The PBRD showed a flat frequency response from 0.1 to 16 kHz. Finally, we present a comparison of the output characteristics of the FMT and PBRD in human cadaveric temporal bones, and show that the PBRD is able to vibrate the RW with higher efficiency than the FMT.

II. THE PBRD DESIGN

A. STRUCTURE OF THE PBRD

The PBRD is installed at the RW niche, like the FMT, but the fixing methods differ (Fig. 1) [26]. Usually, the FMT is wrapped in biological fascia prior to niche positioning, and the entire FMT vibrates [27]. However, the vibrations are not unidirectional, and only some vibrations reach the RW. In contrast, the bottom or side of the PBRD titanium housing is fixed to nearby bone. The PBRD therefore only vibrates at one end, the bellows, and all vibrations reach the RW.

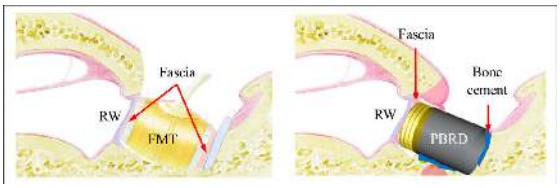

FIGURE 1. The floating mass transducer (FMT) (left) and piezoelectric bellows round window driver (PBRD) (right) installed at the round window (RW) niche [26].

The PBRD structure is shown in Fig. 2(a). The PBRD features a bellows, a ceramic-tip, a piezoelectric element, and a titanium housing. Considering the previous research results on RW-niche volume [28], the overall size of the PBRD was designed to not exceed a maximum outer diameter of 1.75 mm and length of 3 mm [Fig. 2(b)]. When a voltage is applied, the piezoelectric element (fixed to the bottom of the housing) expands or contracts only in the direction of the bellows. To ensure attenuation-free transmission of the piezoelectric displacement to the RW, the vibration membrane must be of low stiffness. Thus, we employed a bellows, not a flat circular membrane, as explained below.

B. MECHANICAL VIBRATIONAL ANALYSIS

The equations yielding the respective spring rates (stiffnesses) of a flat circular membrane and bellows are as

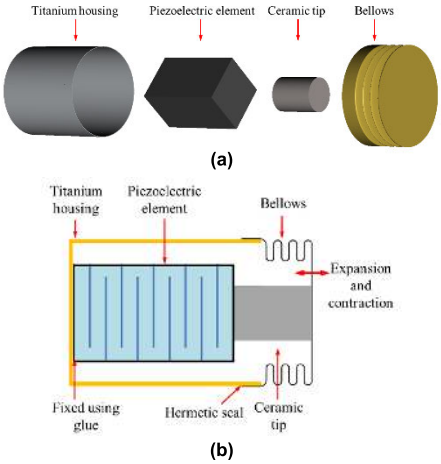

FIGURE 2. (a) The PBRD components and (b) a PBRD cross-section.

follows:

$$k_f = \frac{4.189 E_f t_f^3 f}{\left(1 - v_f^2\right)\left(\frac{D_f}{2}\right)^2} \tag{1}$$

where k_f is the membrane spring rate, E_f is the Young's modulus, t_f is the material thickness, v_f is the Poisson's ratio, and D_f is the outer diameter [29]; and

$$k_b = \frac{1.7 D_b E_b t_b^3 n}{w_b^3 c_f N} \tag{2}$$

where k_b is the bellows spring rate, D_b is the outer diameter, E_b is the Young's modulus, t_b is the material thickness, n is the ply number, w_b is the corrugation height, C_f is a design factor, and N is the number of corrugations [23], [30].

The parameters exerting the greatest influence on stiffness are the material thickness and outer diameter. The membrane stiffness is closely related to the outer diameter, increasing as the diameter decreases and as the material becomes thicker. As the diameter of a flat circular membrane decreases, its stiffness rises markedly because the stiffness is inversely proportional to the square of the diameter [Eq. (1)]. Therefore, a flat circular membrane of high stiffness affords minimal displacement. By contrast, the stiffness of a bellows is directly proportional to the outer diameter, not inversely proportional to the square thereof [Eq. (2)]. Therefore, for smaller diameters the bellows displacement is greater than that of a flat circular membrane.

We subjected both a flat circular membrane and a corrugated bellows to FEA software COMSOL Multiphysics 5.4 (Fig. 3a). The 3D model only represented the components that affect the vibrational analysis. The flat circular membrane and bellows were of identical outer diameter (1.75 mm) and material thickness (7.6 μm). All components were configured using the solid-mechanics routine of the structure-mechanics sub-module, then combined with the ''form union'' command. The material properties of the flat circular membrane (316L stainless steel), bellows

(gold-plated copper), ceramic tip (Al_2O_3), and piezoelectric element (elasticity and coupling matrix of PZT-5H using built-in values) used in the FEA had the following features: a membrane density of 8000 kg/m^3, membrane Poisson's ratio of 0.28; membrane Young's modulus of 128E9 N/m^2, bellows density of 8960 kg/m^3, bellows Poisson's ratio of 0.355, bellows Young's modulus of 119E9 N/m^2, ceramic-tip density of 3800 kg/m^3, ceramic-tip Poisson's ratio of 0.22, ceramic-tip Young's modulus of 375E9 N/m^2. The piezoelectric element was chosen to ensure that the vibrational displacements (160 nm at 3 V_p from 0.1 to 16 kHz) were all directed toward the membrane using the electrostatics routine. The edges of the flat circular membrane, the trim of the bellows, and the bottom of the piezoelectric element were all immobilized using a defined "fixed constraint". The mesh types for the 3D models of the flat circular membrane and bellows were both set to "free tetrahedral". The respective mesh-element parameters for the flat circular membrane and bellows models include maximum element sizes of 0.221 and 0.192 mm, minimum element sizes of 0.0033 and 0.0036 mm, maximum element growth rates of 1.5 and 1.45, curvature factors of 0.6 and 0.5, and narrow-region resolutions of 0.5 and 0.6. The respective meshes of the two models consisted of 65,317 and 150,705 domain elements, 12,020 and 69,790 boundary elements, and 560 and 4,292 edge elements. Solid mechanics and electrostatics were coupled using a piezoelectric-effect routine, and then static and dynamic analyses were performed. The vibrational displacement of the piezoelectric element was transferred (without loss) to the flat circular membrane or the bellows via the cylindrical ceramic tip. The upper panels of Fig. 3(b) show the von Mises stress distributions (based on the static-analysis results) for the flat circular membrane and bellows, with respective surface averages of 1.06E6 and 5.03E5 N/m^2. The respective vibrational displacements calculated at the surface centers [bottom panel of Fig. 3(b)] averaged 140 and 147 nm (based on the dynamic-analysis results). The flat circular membrane reduced the vibrational displacement of the piezoelectric element by approximately 12%, whereas the bellows only reduced it by approximately 8%. In summary, a driver (transducer) featuring a flat circular membrane requires more input voltage to generate the same displacement as a driver employing a bellows. Thus, we incorporated a bellows into our PBRD.

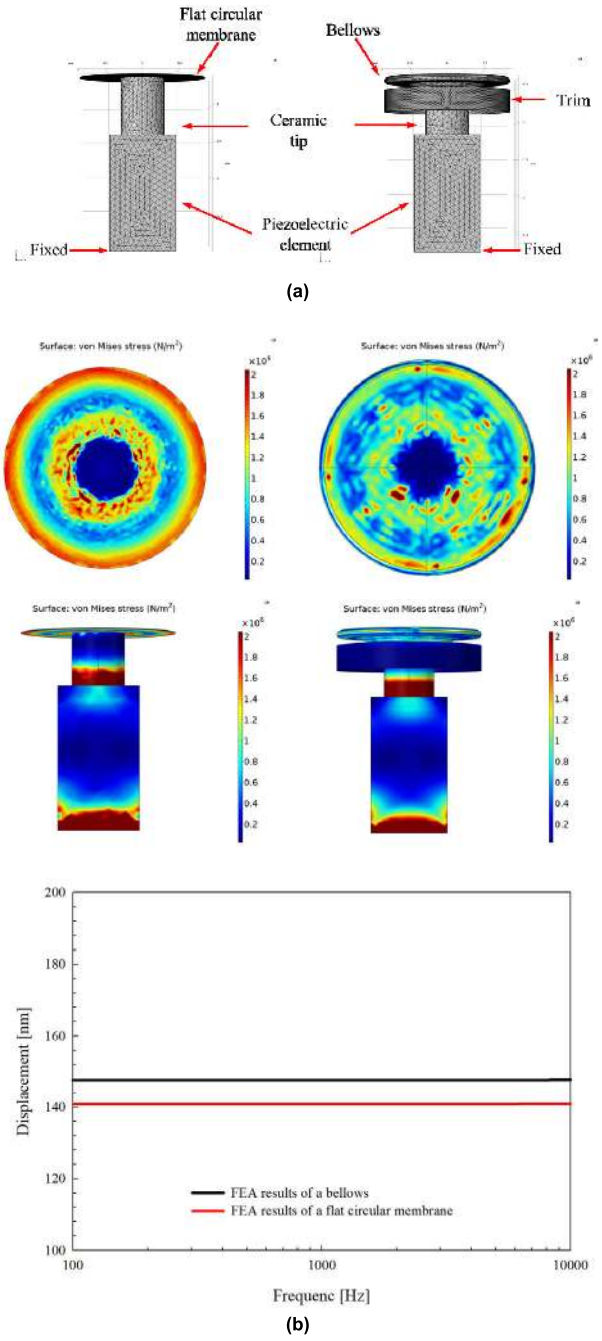

FIGURE 3. (a) Finite element analysis (FEA) models of a flat circular membrane (left) and bellows (right), and (b) the FEA results.

We performed mechanical-vibration analyses to optimize the number of bellows corrugations. The guidelines of the manufacturer (Servometer Inc., Cedar Grove, NJ, USA) indicate that the outer-to-inner diameter ratio should be at least 0.6. For a bellows with an outer diameter of 1.75 mm, the width of one corrugation (i.e., the inner + outer groove widths) must be at least 0.18 mm. In addition, the material thickness should be at least 7.6 μm. Thus informed, we set the outer diameter and thickness to 1.75 mm and 7.6 μm, respectively, and analyzed the frequency-sweep responses when the number of corrugations ranged from one to five (Fig. 4). The input vibration displacement (320 nm at 6 V_p) was that of the piezoelectric element (PAZ-10-0079; Murata Manufacturing Co. Ltd., Kyoto, Japan) used in the PBRD. The use of only one or two corrugations reduced the displacement of the bellows surface by approximately 8% and 5%, respectively. The use of three, four, or five corrugations eliminated the transmission loss (the attenuation). We used three corrugations to minimize the length of the PBRD.

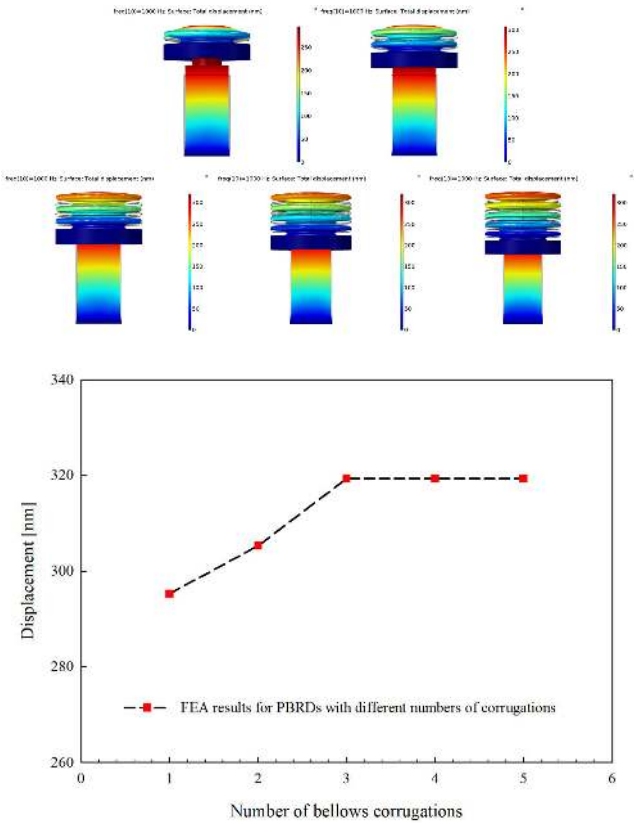

FIGURE 4. Mechanical vibrations (displacement) produced by bellows with different numbers of corrugations.

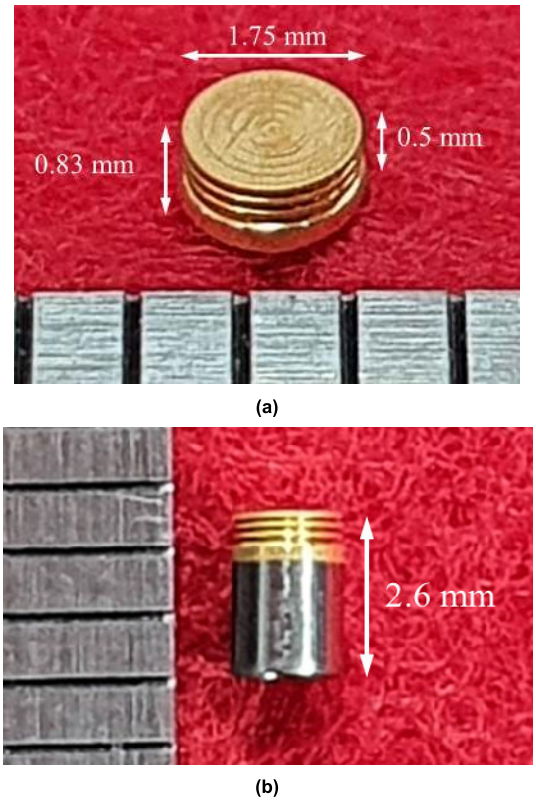

FIGURE 5. (a) The implemented bellows, and (b) the fabricated PBRD.

III. FABRICATION AND TESTING OF THE PBRD

A. FABRICATION OF THE PBRD

We fabricated the optimum bellows as revealed by the FEA results. The vibration-generating piezoelectric element was the PAZ-10-0079 (width 0.9 mm, height 0.9 mm, and depth 1.6 mm) made by Murata Manufacturing Co. Ltd. The bellows was custom-made by Servometer Inc., guided by the FEA data. The bellows shape is that of the analytical model in Fig. 5(a). The outer diameter is 1.75 mm, the height is 0.5 mm (excluding the trim height), the thickness is 7.6 μm, and the bellows has three corrugations. The bellows was fabricated from copper and then covered with gold; thus, it cannot be affected by an external magnetic field. A titanium housing (diameter 1.75 mm and length 2.1 mm) and a ceramic tip (diameter 0.6 mm and length 0.8 mm) were machined. The PBRD was meticulously assembled under a microscope [Fig. 5(b)]. The bottom of the piezoelectric element was glued to the inner bottom of the titanium housing using cyanoacrylate. The elements, ceramic tip, and bellows were similarly glued together, and cyanoacrylate was employed to seal the bellows trim to the outer wall of the titanium housing.

We assessed the frequency-response characteristics of the PBRD by measuring its vibrations using a fast Fourier-transform (FFT)-based data acquisition system (consisting of an NI PXI-4461 board operating in an NI PXI-1042 chassis made by National Instruments Corp., Austin, TX, USA) with a 96-kHz sampling rate and 8,192 FFT points, and a laser Doppler vibrometer (LDV; i.e., an OFV-551 sensor head and OFV-5000 controller made by Polytec GmbH, Waldbronn, Germany). Sinusoidal signals drove the PBRD and the LDV measured the vibrations, with the PBRD operating under the no-load condition. The bottom of the PBRD housing was fixed to an anti-vibration table (using cyanoacrylate glue) to ensure that all vibrations generated by the piezoelectric element reached the bellows. The measurement system then applied a constant voltage (6 V_p) to the PBRD. The frequency-response characteristics were measured by the LDV aimed at the center of the bellows surface (Fig. 6). The frequency-response characteristics of the PBRD (red line) and piezoelectric element (black line) were nearly identical, which confirms the FEA prediction of no attenuation of the piezoelectric vibration. In addition, to verify the FEA result, it was compared against the frequency response for a version of the device manufactured with a flat circular membrane (blue line). When compared with the frequency response characteristics of PBRD, it was confirmed that the output magnitude of all frequency bands was reduced by an average of 15%.

B. CADAVERIC EXPERIMENTS

To verify the usefulness of the PBRD, we compared its output characteristics to those of an FMT using human cadaveric

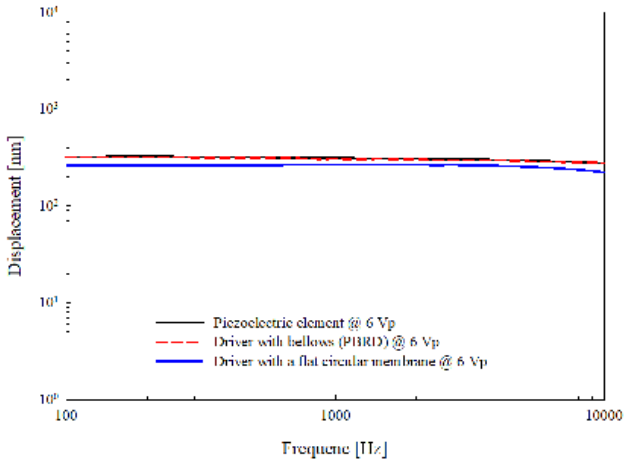

FIGURE 6. **No-load frequency-response characteristics of the piezoelectric element, the driver with bellows (PBRD), and the driver with a flat circular membrane, for a 6 V_p stimulus.**

temporal bones. These experiments were conducted at the OtoBiomechanics Laboratory of the Massachusetts Eye & Ear in Boston, MA, USA. Custom LabVIEW-based (National Instruments Corp.) measurement software (SyncAv version 0.30) was used to control the data acquisition hardware in order to generate a sequence of tones from 0.1 to 16 kHz to drive either an ear-canal speaker or the transducer under test, and then record measurements of the stapes velocity from the LDV and, for the sound-driven measurements, the pressure in the ear canal using a probe-tube microphone (ER-7c, Etymotic Research, Inc., Elk Grove Village, IL, USA). The experimental setup is shown in Fig. 7.

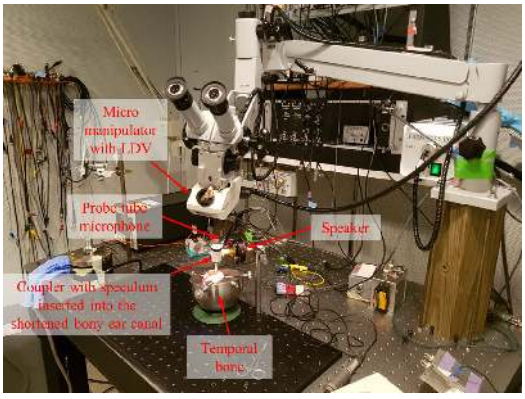

FIGURE 7. **Measurement setup using human temporal bones.**

Five normal human temporal bones (TBs) with no history of ear disease (TB1–5) were used. Each was harvested and frozen within 24 h of death, then thawed before use in the experiments. A mastoidectomy was performed on each bone to open the facial recess and provide access to the RW niche. The bony overhang around the perimeter of the RW membrane was reduced to facilitate coupling of the PBRD and FMT to the RW membrane. To establish the baseline sound-driven response of each TB, sound was presented via a speaker coupled to a speculum inserted into the shortened bony ear canal and the sound pressure near the eardrum was measured with the probe-tube microphone. The velocity of the stapes in response to an ear-canal sound pressure of 94 dB SPL (1 Pa) was measured using the LDV (Fig. 8). The upper and lower limits from the ASTM F2504-05 standard, relevant to evaluating implantable hearing aids using TBs, are also shown for comparison (red dotted lines). The measured stapes responses from the five TBs fall mostly within this reference range up through 4 kHz.

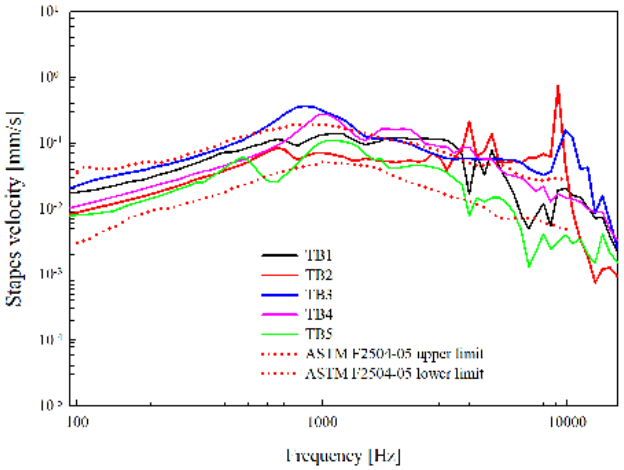

FIGURE 8. **Stapes-velocity measurements in five temporal bones (TB1–5), as driven by a 94-dB-SPL (1 Pa) acoustic stimulus in the ear canal.**

To ensure that the PBRD transmitted vibrations to the RW, it was positioned between the RW and inferior hypotympanic wall. To minimize damage to the RW membrane and to better couple its vibrations to the RW, soft tissue was placed between the RW membrane and the PBRD. The non-moving end of the PBRD housing was fixed to the inferior bony wall using bone wax. After applying a constant 6 V_p stimulus to the PBRD, the stapes velocity was measured using the LDV. To confirm that the PBRD output was linear, all measurements were repeated with the applied voltage decreased in 10-dB steps (i.e., 6, 2, 0.67, and 0.2 V_p). The PBRD was then carefully removed without damaging the RW membrane, and the FMT was positioned in the same location. To stabilize the position of the FMT, soft Jeltrate material (Dentsply Caulk, Milford, DE, USA) was placed between the free end of the FMT and the hypotympanic bony wall, which allowed the whole FMT to vibrate. The experiment was repeated with voltages varying from 0.3 to 0.01 V_p, in decreasing 10-dB steps (i.e., 0.3, 0.1, 0.033, and 0.01 V_p). Fig. 9 plots the frequency responses for the two transducer types at the various input voltages for all five TBs. Fig. 10 presents the data of Fig. 9 in terms of velocity versus voltage for selected frequencies, thus illustrating the linearity characteristics of the PBRD and FMT. Specifically, the plot shows the average stapes velocity of the five TBs at six octave-spaced frequencies from 0.5 to 16 kHz.

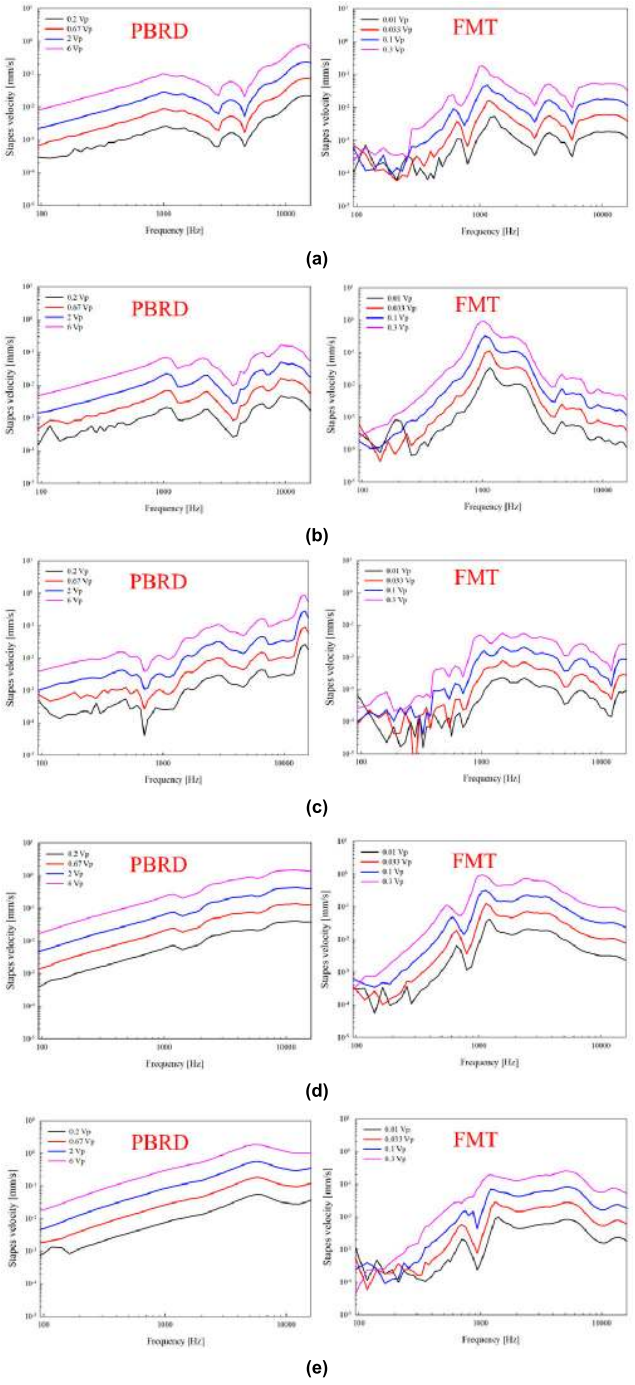

FIGURE 9. Stapes-velocity frequency-response characteristics when the RW was stimulated with the aid of the PBRD and FMT for (a) TB1, (b) TB2, (c) TB3, (d) TB4, and (e) TB5.

IV. DISCUSSION AND SUMMARY

We here describe a novel transducer for stimulating the RW, the PRBD, which is expected to be unaffected by environmental magnetic fields. To ensure that the displacements of its piezoelectric element were not attenuated on their way to the RW, we used a nonmagnetic copper-based bellows of low stiffness. With the aid of FEA, we compared the vibration-transmission efficiencies of the bellows against a design with a flat circular membrane and found that the bellows design was superior. We bench-tested the PBRD under no-load conditions and confirmed its theoretical frequency-response characteristics. We additionally measured the output characteristics of the PBRD and FMT characteristics using TBs. As shown in Fig. 10, the PBRD, like the FMT, satisfies an essential characteristic of a transducer; i.e., the output varies linearly with respect to the input voltage.

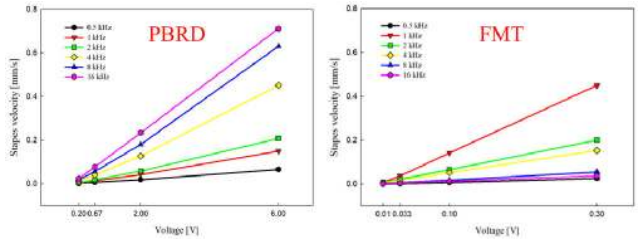

FIGURE 10. Linearity metrics of the PBRD and FMT for various frequencies based on the results in Fig. 9. The plotted stapes-velocity values are averaged from all five TBs.

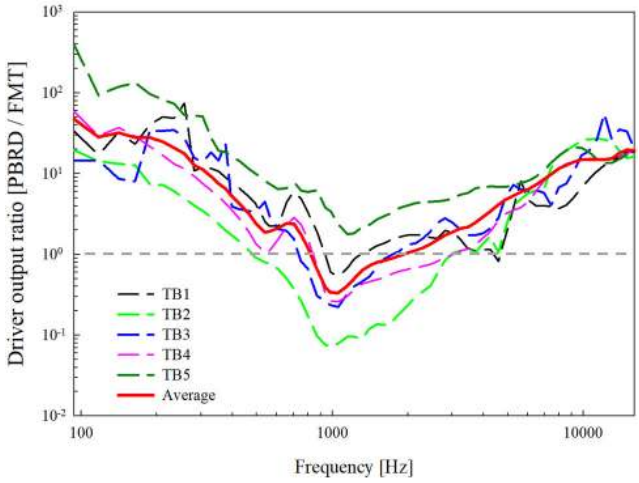

FIGURE 11. Ratio of the PBRD to FMT output for each TB. The PBRD outperforms the FMT when the lines are above the gray dashed line, and worse when below it.

The output magnitudes of the PBRD and FMT are compared for the TB tests by plotting the PBRD/FMT ratios (Fig. 11). The solid red line is the average output ratio for all TBs (TB1–5). The PBRD output was higher than that of the FMT for all frequencies, on average, except for the 0.8 to 2 kHz range where the FMT resonated and did better. However, as a fixed-type transducer, the PBRD transmits its vibrations to the RW more efficiently than the floating-mass type of the FMT, and the PBRD output characteristics were excellent in the low-frequency region (solid red line in Fig. 11). The PBRD output was also higher than the FMT at frequencies above 2 kHz, which is a beneficial range for enhancing speech recognition and treating high-frequency

sensorineural hearing loss. In conclusion, the PBRD has the advantages of not being affected by external magnetic fields, and having better frequency-response characteristics than conventional RW drivers. However, as shown in Fig. 11, the output magnitude of the PBRD is somewhat lower than that of the FMT in the mid-band region (0.8–2 kHz). To improve the performance of the PBRD, we will exploit mechanical resonance to increase its mid-band output and reduce its driving voltage.

REFERENCES

[1] T. M. Eßinger, M. Koch, M. Bornitz, N. Lasurashvili, M. Neudert, and T. Zahnert, "Sensor-actuator component for a floating mass transducer-based fully implantable hearing aid," *Hearing Res.*, vol. 378, pp. 157–165, Jul. 2019.

[2] D. H. Shin, K. W. Seong, S. Puria, K.-Y. Lee, and J.-H. Cho, "A tri-coil bellows-type round window transducer with improved frequency characteristics for middle-ear implants," *Hearing Res.*, vol. 341, pp. 144–154, Nov. 2016.

[3] S. Labassi, M. Beliaeff, V. Péan, and P. Van de Heyning, "The vibrant soundbridge middle ear implant: A historical overview," *Cochlear Implants Int.*, vol. 18, no. 6, pp. 314–323, Nov. 2017.

[4] U. A. Gamm, M. Grossöhmichen, R. B. Salcher, N. K. Prenzler, T. Lenarz, and H. Maier, "Optimum coupling of an active middle ear actuator: Effect of loading forces on actuator output and conductive losses," *Otology Neurotology*, vol. 40, no. 6, pp. 789–796, Jul. 2019.

[5] A. L. Gesing, Z. N. Masson, D. C. Arellano, F. Alves, S. Paul, and J. A. Cordioli, "Middle ear ossicular chain vibration detection by means of an optimized MEMS piezoelectric accelerometer," *IEEE Sensors J.*, vol. 19, no. 6, pp. 2079–2086, Mar. 2019.

[6] M. D. Seidman, T. A. Janz, and J. A. Shohet, "Totally implantable active middle ear implants," *Otolaryngolog. Clinics North Amer.*, vol. 52, no. 2, pp. 297–309, Apr. 2019.

[7] J. A. Shohet, D. M. Gende, and C. S. Tanita, "Totally implantable active middle ear implant: Hearing and safety results in a large series," *Laryngoscope*, vol. 128, no. 12, pp. 2872–2878, Dec. 2018.

[8] D. Calero, S. Paul, A. Gesing, F. Alves, and J. A. Cordioli, "A technical review and evaluation of implantable sensors for hearing devices," *Biomed. Eng. OnLine*, vol. 17, no. 1, p. 23, Feb. 2018.

[9] D. Shin and J.-H. Cho, "Piezoelectric actuator with frequency characteristics for a middle-ear implant," *Sensors*, vol. 18, no. 6, p. 1694, May 2018.

[10] D. S. Haynes, J. A. Young, G. B. Wanna, and M. E. Glasscock, "Middle ear of implantable hearing devices: An overview," *Trends Amplification*, vol. 13, no. 3, pp. 206–214, Sep. 2009.

[11] F. F. Brkic, D. Riss, A. Auinger, B. Zoerner, C. Arnoldner, W.-D. Baumgartner, W. Gstoettner, and E. Vyskocil, "Long-term outcome of hearing rehabilitation with an active middle ear implant," *Laryngoscope*, vol. 129, no. 2, pp. 477–481, Feb. 2019.

[12] S. Monini, A. Bianchi, R. Talamonti, F. Atturo, C. Filippi, and M. Barbara, "Patient satisfaction after auditory implant surgery: Ten-year experience from a single implanting unit center," *Acta Oto-Laryngologica*, vol. 137, no. 4, pp. 389–397, Apr. 2017.

[13] T. R. McRackan, W. B. Clinkscales, J. B. Ahlstrom, S. A. Nguyen, and J. R. Dubno, "Factors associated with benefit of active middle ear implants compared to conventional hearing aids," *Laryngoscope*, vol. 128, no. 9, pp. 2133–2138, Sep. 2018.

[14] S. Busch, T. Lenarz, and H. Maier, "Comparison of alternative coupling methods of the vibrant soundbridge floating mass transducer," *Audiology Neurotology*, vol. 21, no. 6, pp. 347–355, Jan. 2017.

[15] A. Müller, P. Mir-Salim, N. Zellhuber, R. Helbig, M. Bloching, T. Schmidt, S. Koscielny, O. C. Dziemba, S. K. Plontke, and T. Rahne, "Influence of floating-mass transducer coupling efficiency for active middle-ear implants on speech recognition," *Otology Neurotology*, vol. 38, no. 6, pp. 809–814, Jul. 2017.

[16] J. Wales, K. Gladiné, P. Van de Heyning, V. Topsakal, M. von Unge, and J. Dirckx, "Minimally invasive laser vibrometry (MIVIB) with a floating mass transducer—A new method for objective evaluation of the middle ear demonstrated on stapes fixation," *Hearing Res.*, vol. 357, pp. 46–53, Jan. 2018.

[17] T. Chen, L.-J. Ren, D.-M. Yin, J. Li, L. Yang, P.-D. Dai, and T.-Y. Zhang, "A comparative study of MED-EL FMT attachment to the long process of the incus in intact middle ears and its attachment to disarticulated stapes head," *Hearing Res.*, vol. 353, pp. 97–103, Sep. 2017.

[18] T. Lenarz, D. Zimmermann, H. Maier, and S. Busch, "Case report of a new coupler for round window application of an active middle ear implant," *Otology Neurotology*, vol. 39, no. 10, pp. e1060–e1063, Dec. 2018.

[19] A. Arnold, C. Stieger, C. Candreia, F. Pfiffner, and M. Kompis, "Factors improving the vibration transfer of the floating mass transducer at the round window," *Otology Neurotology*, vol. 31, no. 1, pp. 122–128, Jan. 2010.

[20] M. Müller, R. Salcher, T. Lenarz, and H. Maier, "The hannover coupler: Controlled static prestress in round window stimulation with the floating mass transducer," *Otology Neurotology*, vol. 38, no. 8, pp. 1186–1192, Sep. 2017.

[21] H. Liu, H. Wang, Z. Rao, J. Yang, and S. Yang, "Numerical study and optimization of a novel piezoelectric transducer for a round-window stimulating type middle-ear implant," *Micromachines*, vol. 10, no. 1, p. 40, Jan. 2019.

[22] B. Schwab, S. Grigoleit, and M. Teschner, "Do we really need a coupler for the round window application of an AMEI?" *Otology Neurotology*, vol. 34, no. 7, pp. 1181–1185, Sep. 2013.

[23] D. H. Shin and J.-H. Cho, "Design and development of a tri-coil bellows transducer for RW-drive implantable middle-ear hearing aid using FEA," *IEEE/ASME Trans. Mechatronics*, vol. 23, no. 3, pp. 1436–1444, Jun. 2018.

[24] J. H. Wagner, A. Ernst, and I. Todt, "Magnet resonance imaging safety of the vibrant soundbridge system: A review," *Otology Neurotology*, vol. 32, no. 7, pp. 1040–1046, Sep. 2011.

[25] I. Todt, P. Mittmann, A. Ernst, S. Mutze, and G. Rademacher, "*In vivo* experiences with magnetic resonance imaging scans in vibrant soundbridge type 503 implantees," *J. Laryngology Otology*, vol. 132, no. 5, pp. 401–403, May 2018.

[26] A. M. Beltrame, I. Todt, G. Sprinzl, M. Profant, and B. Schwab, "Consensus statement on round window vibroplasty," *Ann. Otology, Rhinology Laryngology*, vol. 123, no. 10, pp. 734–740, Oct. 2014.

[27] L. Edfeldt and H. Rask-Andersen, "Round window vibroplasty in chronic ear surgery: Comparison with conventional hearing rehabilitation," *Acta Oto-Laryngologica*, vol. 133, no. 8, pp. 814–825, Aug. 2013.

[28] M. Shakeel, P. M. Spielmann, S. E. Jones, and S. S. M. Hussain, "Direct measurement of the round window niche dimensions using a 3-dimensional moulding technique—A human cadaveric temporal bone study," *Clin. Otolaryngology*, vol. 40, no. 6, pp. 657–661, Dec. 2015.

[29] B. Balachandran and E. B. Magrab, *Vibrations*. New York, NY, USA: Cambridge Univ. Press, 2018.

[30] C. Becht, "An evaluation of EJMA stress calculations for unreinforced bellows," *J. Pressure Vessel Technol.*, vol. 124, no. 1, pp. 124–129, Feb. 2002.

DONG HO SHIN received the B.S. degree in electronics engineering from Dongseo University, Busan, South Korea, in 2009, and the M.S. and Ph.D. degrees from the School of Electronics Engineering, Kyungpook National University, South Korea, in 2011 and 2016, respectively.

From 2016 to 2019, he was a Research Fellow with the Institute of Biomedical Engineering Research, Kyungpook National University, where he is currently a Research Professor with the Institute of Biomedical Engineering Research. His research interests include the electronic and mechanical system of medical instruments and middle-ear implants transducer.

KI WOONG SEONG received the B.S. degree in electronics engineering, and the M.S. and Ph.D. degrees in electronics engineering from Kyungpook National University, Daegu, South Korea, in 1998, 2000, and 2010, respectively.

From 2010 to 2011, he was a Research Professor with the Institute of Biomedical Engineering Research, Kyungpook National University. Since 2012, he has been a Professor with the Department of Biomedical Engineering, Kyungpook National University Hospital, South Korea. His research interests include implantable hearing aids, bioelectronics, biomedical signal processing, and sensor applications in biomedical instrumentations.

HIDEKO HEIDI NAKAJIMA received the B.S., M.S., and Ph.D. degrees in biomedical engineering from the Boston University College of Engineering, Boston, MA, USA, and the M.D. degree from the Boston University School of Medicine. She is currently an Associate Professor of otolaryngology head and neck surgery with the Harvard Medical School. She conducts research at the Eaton-Peabody Laboratories of the Massachusetts Eye and Ear Infirmary, Boston, MA, USA. Her interests include addressing fundamental scientific questions about the auditory systems, and developing new and improved methods to diagnose and treat human hearing disease. Her primary research involves human auditory mechanics, middle-ear prostheses, and acoustical stimulation of the cochlea.

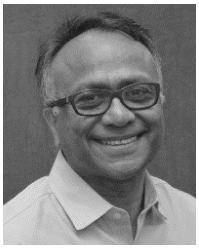

SUNIL PURIA received the B.E.E.E. degree from the City College of New York, in 1983, the M.S. degree from Columbia University, New York, in 1985, and the Ph.D. degree from the City University of New York, in 1991. He did most of his Ph.D. thesis work at AT&T Bell Labs, Murray Hills, NJ, USA. He then went on to do a Post-doctoral Fellowship at the Massachusetts Institute of Technology (MIT), Cambridge. He was an Adjunct Faculty Member at Harvard University Medical School until 1997. He is currently an Engineer-Scientist, holding dual positions at Stanford University as an Associate Professor (Consulting) with the Department of Mechanical Engineering and the Department of Otolaryngology-HNS, and as the Chief Scientist at EarLens Corporation. He is also an Associate Professor of otolaryngology head and neck surgery with the Harvard Medical School, and conducts research at the Eaton-Peabody Laboratories of the Massachusetts Eye and Ear Infirmary, Boston, MA, USA. He was the Chair of the Middle-Ear Mechanics in Research in Otology (MEMRO) 2009 International meeting at Stanford University. His areas of specialty are biomechanics, physiology, imaging of the auditory systems, and novel hearing aid technologies.

JIN-HO CHO (Senior Member, IEEE) received the B.S. degree in electrical engineering, and the M.S. and Ph.D. degrees in electronics engineering from Kyungpook National University, Daegu, Korea, in 1977, 1979, and 1988, respectively. He was a Visiting Professor with the Department of Biomedical Engineering, College of Engineering, University of Iowa, USA, in 1991. From 1984 to 2008, he was the Head of the Department of Biomedical Engineering. He was associated with Kyungpook National University Hospital and School of Medicine. From 1984 to 2018, he was a Professor of the School of Electronics Engineering, College of IT Engineering, Kyungpook National University. In 2012, he served as the Chairman for the Korea Society of Medical & Biological Engineering. He currently works as a Research Professor with the Institute of Biomedical Engineering Research, Kyungpook National University, South Korea. His main research interest is transducer design for middle-ear implants, and other interests are including biomedical signal processing and sensor applications in biomedical instrumentations.